# Precision molecular spectroscopy with a phase-locked terahertz quantum-cascade laser

N.B. When citing this work, cite the original published paper.

(article starts on next page)

# Precision molecular spectroscopy with a phase-locked terahertz quantum-cascade laser

**R. VOIGT,**[1,2,*] **M. WIENOLD,**[1] **D. JAYASANKAR,**[3] **J. STAKE,**[3] ⓘ **X. LÜ,**[4] **K. BIERMANN,**[4] **AND H. W. HÜBERS**[1,2]

[1]*German Aerospace Center (DLR), Institute of Optical Sensor Systems, Rutherfordstr. 2, 12489 Berlin, Germany*
[2]*Humboldt-Universität zu Berlin, Department of Physics, Newtonstr. 15, 12489 Berlin, Germany*
[3]*Terahertz and Millimeter Wave Laboratory, Department of Microtechnology and Nanoscience (MC2), Chalmers University of Technology, SE-412 96 Göteborg, Sweden*
[4]*Paul-Drude-Institut für Festkörperelektronik, Leibniz-Institut im Forschungsverbund Berlin e. V., Hausvogteiplatz 5–7, 10117 Berlin, Germany*
[*]*Robert.Voigt@dlr.de*

**Abstract:** We demonstrate precision molecular spectroscopy with a phase-locked quantum cascade laser (QCL) over its entire frequency tuning range at 3.4 THz. A Schottky diode harmonic mixer is used to mix the QCL emission with a multiplied microwave signal, referenced to a rubidium frequency standard, to create an intermediate frequency (IF) signal, which is used to phase-lock the QCL. Tuning the frequency of the multiplied microwave reference and keeping the IF fixed allows for precise frequency control of the laser. We identify ten methanol transitions between 3443.5 and 3447.6 GHz and quantify the transition frequencies and broadening parameters with high precision. These measurements are performed without liquid cryogens in a compact setup.

## 1. Introduction

High-resolution terahertz spectroscopy is used in scientific fields such as astronomy and atmospheric research, as many atoms and molecules exhibit radiative transitions in the terahertz (THz) range [1–4]. To identify these transitions, molecular data catalogs, for example, the high-resolution transmission molecular absorption database (HITRAN) and the molecular data catalog from Jet Propulsion Laboratory (JPL), are needed. These databases rely on measured data as well as molecular models to predict transition frequencies and line strengths [5]. To validate the catalog data and the underlying models, precise measurements with absolute frequency accuracy are required. There are several methods to perform THz precision spectroscopy such as backward-wave oscillator-based (BWO) spectroscopy, cavity-enhanced absorption spectroscopy using an amplifier multiplier chain (AMC) [6], frequency-comb-assisted THz spectroscopy [7,8] or spectroscopy using difference frequency generation (DFG) [9,10]. All of these methods require monochromatic sources with extremely small linewidths. BWOs are electronically tunable sources that, combined with frequency stabilization, can be used to perform sensitive broadband measurements [11]. Cavity-enhanced absorption spectroscopy uses the monochromatic output of an AMC and a high-finesse cavity to increase the optical path length and measure weakly absorbing molecular species. Frequency-comb-assisted THz spectroscopy is based on phase-locking of a quantum-cascade laser (QCL) to the line of a frequency comb generated by a mode-locked femtosecond laser. Another way to generate a frequency-stable signal is by photomixing two distributed feedback (DFB) lasers, locked to an optical cavity or frequency standard, to generate the difference frequency [9,10]. DFG techniques allow precise frequency control over large

frequency ranges from 1 to 7.5 THz with powers under one microwatt [10]. In this work we phase-lock a QCL to an external reference signal by mixing it with the emission of an AMC. Single-mode THz QCLs are designed to operate in the range of 2-5 THz and offer high output power in the mW range in combination with a small linewidth [12,13]. Due to these optical properties, they are also used as local oscillators in heterodyne receivers [3,14]. By mixing the QCL emission with a multiplied microwave signal, we are able to downconvert it to the MHz range and phase-lock it to an electronically generated reference signal. This allows for precise control of the frequency of the QCL over its whole operating range with respect to a primary frequency standard. We characterize several transitions of methanol, as it is an important tracer of fundamental constants [15]. In order to enable easy operation of the spectrometer, we use a mechanical cryocooler rather than a liquid-helium cryostat for operation of the QCL and a Golay detector operating at room-temperature.

## 2. Experimental setup

The experimental configuration of the spectroscopy setup is shown in Fig. 1(a). The 3.4-THz QCL is based on GaAs/Al$_x$Ga$_{1-x}$As heterostructures, in which a bound-to-continuum lasing transition is combined with a fast transition resonant to the energy of the longitudinal optical (LO) phonon. The system was fabricated from the same wafer as sample B of Ref. [16]. The wafer was grown using molecular beam epitaxy on a semi-insulating GaAs substrate and single-mode operation was achieved by using a short Fabry-Pérot resonator. The Light-current-voltage characteristics for the laser and its emission spectra at different currents are shown in Fig. 2 (a) and (b) respectively. It is operated at a temperature of 47 K, while a proportional-integral-derivative (PID) loop provides a stability of ± 2 mK. Special care has been taken to reduce optical feedback effects related to mechanical vibrations. Where possible, the surfaces of the optical components are positioned at slight angles to reduce any unwanted back reflections. An aperture is placed between the QCL and the wire grid polarizer at an angle of roughly 45 °, with respect to the light beam, to minimize reflections of the harmonic mixer. Additionally, the window of the mechanical cryocooler has been fixated tightly to minimize feedback effects due to cooler vibrations. Most of the linearly polarized emission of the QCL is collimated by a polymethylpentene (TPX) lens with a focal length $f$ = 45 mm into a 35 cm long absorption cell filled with methanol, while about 10% is reflected by a wire grid polarizer and focused onto a harmonic Schottky diode mixer [17] by another TPX lens ($f$ = 34 mm). The mixer used has been designed and fabricated at Chalmers University of Technology and is further described in [18]. The gas pressure inside
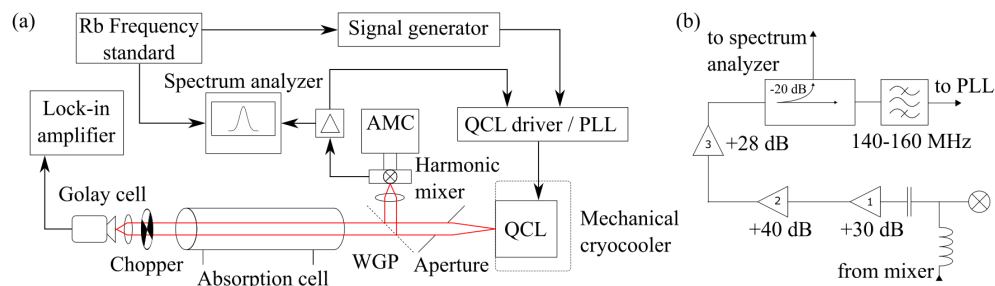


**Fig. 1.** (a) Experimental setup for high-precision molecular spectroscopy (QCL: quantum-cascade laser, WGP: wire grid polarizer, PLL: phase-locked loop, AMC: amplifier multiplier chain). (b) IF signal amplification, coupling and filtering. The amplifiers used are 1: LNA-30-00100400-13-10P Narda-MITEQ, 2: LNA-40-00100400-13-10P Narda-MITEQ and 3: ZHL-1042J+ Mini-Circuits, along with directional coupler ZFDC-20-33-S+ Mini-Circuits and bandpass SBP-150+ Mini-Circuits.

the absorption cell is measured using a capacitive pressure sensor (Pfeiffer Vacuum CMR372). The transmitted QCL signal that passed the absorption cell is then modulated by a chopper at 30 Hz and detected with a Golay cell in combination with a lock-in amplifier (Stanford Research Systems SR865A). The QCL emission, which is reflected away from the absorption cell, is mixed with the 6th harmonic of a 574-GHz signal, which is generated by an AMC from a microwave source (VDI, Tx 249) of 11.97 GHz. The downconverted intermediate frequency (IF) signal is amplified by a chain of three low noise amplifiers as shown in Fig. 1(b). The main part of the signal is used for frequency stabilization via a phase-locked loop (PLL) circuit (QubeCL) by using a directional coupler, while a small portion is measured with a spectrum analyzer (Keysight N9010A). A bandpass operating from 140 MHz to 160 MHz is used to further reduce the noise of the IF signal for the PLL circuit. The PLL circuit locks the IF signal to a 145 MHz reference signal, that is provided by a signal generator (TTi TGF4242). By tuning the reference frequency of the AMC while keeping the QCL locked to the 145 MHz signal, the QCL can be tuned over its entire frequency range of 4.65 GHz at 47 K. The QCL frequency is tuned exclusively by the current while the temperature is stabilized by a temperature controller. The frequency range is dependent on the temperature as the current threshold of the QCL changes. The timebases of the AMCs, the signal generators, the lock-in amplifier, and the spectrum analyzer in this setup have been synchronized to a 10-MHz rubidium (Rb) frequency standard (Quartzlock E80-GPS). The full width at half maximum (FWHM) of the QCL emission has been determined to 325 kHz. Amplitude fluctuations of the detector signal caused by the interplay of QCL current and intensity arise as the QCL frequency is locked. These fluctuations are observed in the time-resolved detector signal, but due to the long integration time of 0.1 s it neither affects the SNR nor the sensitivity of our measurements.
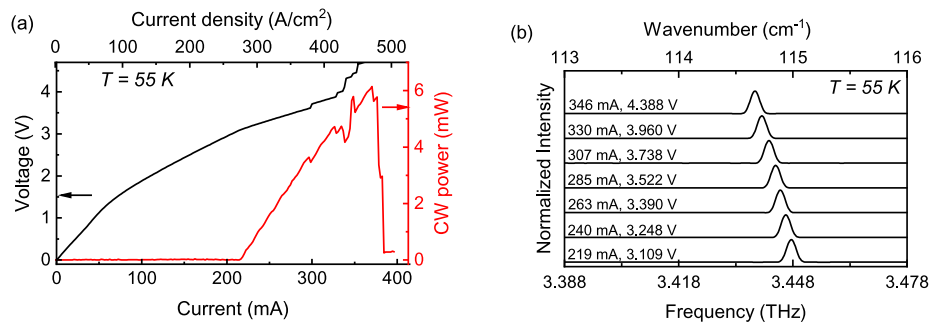


**Fig. 2.** (a) Light-current-voltage characteristics for the QCL and (b) QCL emission spectra at different currents under continuous-wave (CW) operation at 55 K.

Each methanol transition with a frequency accessible by the QCL is measured individually over a range of 200 to 300 MHz at several pressures. To ensure reproducibility and comparability between the measurements, the following procedure has been used. Before each single measurement, the absorption cell was flooded with methanol up to its saturation vapor pressure of 128 mbar for one minute. The absorption cell was then evacuated down to the desired pressure value and the valve was closed followed by a two-minute waiting period to avoid transient effects. After that period, the frequency sweep was started. Measurements of the transitions had a sweep range of 200 to 300 MHz and a stepsize of 200 kHz resulting in measurement periods of roughly 2 minutes per pressure value and transition with an integration time of 0.1 s per step. The resulting tuning speed of 2 MHz/s is low enough that the drift correction of the QCL controller is able to keep the QCL locked continuously. The measuring time for each sequence is primarily limited by the leakage rate of the absorption cell of roughly 0.9 mbar per hour yielding pressure uncertainties. The total measuring time is further limited to about 60 minutes, to keep the baseline sufficiently

stable for the fit of the lineshape. This does not allow for an evacuation of the absorption cell until complete disappearance of the methanol lines during the measurements. As the transitions are measured individually, instead of all at once, we fitted each sequence individually rather than by using multispectral fitting [19]. Instead of performing a reference scan with an empty gas cell, we fitted the background signal by using the data obtained at the lowest pressure, excluding a range of ± (20-50) MHz around the center frequency of each peak. This background fit was then fixed for all measurements regarding that transition, and the absorption profile was fitted using a Voigt profile. A Voigt profile, which is a convolution of a Gaussian and Lorentzian, is chosen as it reflects both collisional (Lorentzian) and thermal (Gaussian) broadening. The Lorentzian and Gaussian widths were then used to calculate the FWHM and the pressure broadening. As expected, the Gaussian width stayed constant at roughly 7.55 MHz, only affected by the Doppler broadening of methanol and the laser frequency, while the Lorentzian width was affected by the pressure broadening. Typical residuals of one of the measurements can be seen in the lower panel of Fig. 3(a).
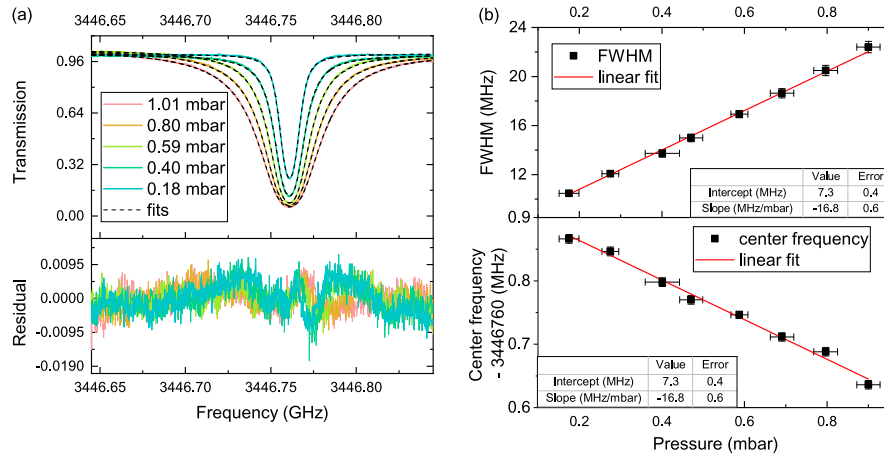


**Fig. 3.** (a) Transmission of the $(J,(\pm)K,(\pm)\nu_t) = (4,3,+2)\leftarrow(5,4,-1)$ transition of methanol at different pressures and Voigt profile fits (upper panel). Residuals of the transmission data (lower panel). (b) FWHM (upper panel) and center frequency (lower panel) of the same transition as a function of the pressure.

## 3.  Results and discussion

Figure 3(a) shows the $(4,3,+2)\leftarrow(5,4,-1)$ (no. 8 in Table 1) transition of methanol at different pressures. The quantum number format used in this work is $(J, (\pm)K$, parity $(\pm)$ and $\nu_t)$. Parity is noted as '+' or '−' for A-state transitions, while E1 and E2 states are indicated by positive (unsigned) and negative signs of K, respectively. The center frequency of this transition has been determined by fitting a Voigt profile and is presented in Fig. 3(b) as a function of pressure. By using the linear fit of the center frequencies, the rest frequency $f_{\text{rest}}$ is determined as the intercept at 0 mbar. These measurements have been performed for all transitions in the spectral range of 3443.5 GHz to 3447.6 GHz, as presented in Fig. 4. The rest frequencies as well as their pressure shifts, broadening parameters, and line strengths are presented in Table 1. To derive the line strength from the transmission, the absorption coefficient is calculated. The absorption coefficient includes the pressure of the gas, the Boltzman constant, the line shape, and the line intensity. As the other quantities are given, we can calculate the line intensity and, by using a unit conversion multiplier, we can depict the line strength in the same format as the JPL catalog for better comparison. The frequency difference between the rest frequency $f_{\text{rest}}$ and the frequency
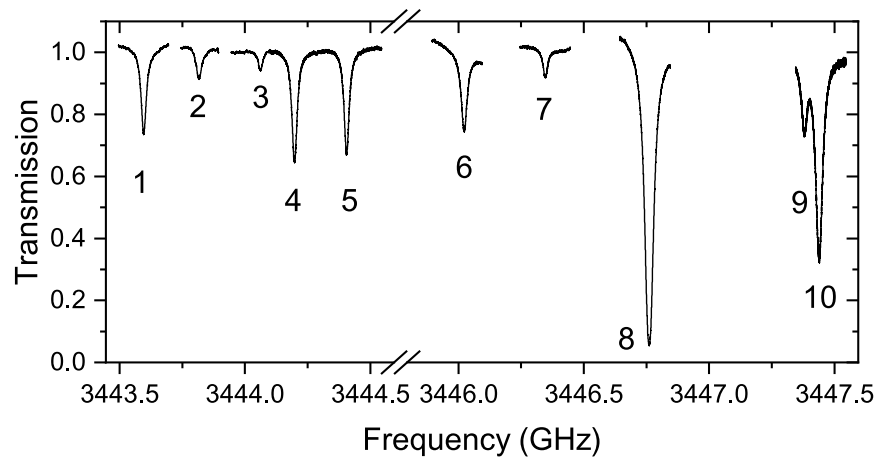
**Fig. 4.** Measured transitions of methanol at about 1.0 mbar.

given by the JPL catalog, $f_{JPL}$, is given as $\Delta f = f_{rest} - f_{JPL}$. The same comparison is performed with data from Ref. [20], presented as $\Delta f_M$ in Table 1. Transitions 1 and 9 in Table 1 have been measured as single transitions, while they consist of two transitions each, according to the JPL catalog, since the Doppler broadening of 7.55 MHz is greater than the frequency difference of these single transitions. In these cases, the frequency difference to both JPL frequencies are given. For most transitions, the determined rest frequencies differ less than 1 MHz from the rest frequencies given by the JPL catalog [21]. For weakly absorbing transitions 2, 3 and 7 at 3443.8 GHz, 3444.1 GHz and 3446.3 GHz, respectively, these differences increase up to 6 MHz. The accuracy of the models used for these catalogs is limited by the experimental input data. As stronger transitions exhibit smaller uncertainties due to higher signal-to-noise ratio, the models predict these stronger transitions with higher accuracy compared to weakly absorbing transitions. For transition 3, the pressure shift and pressure broadening could not be determined due to high uncertainties from the fits. The measured line strengths of the transitions match fairly well with the values of the JPL catalog with slight differences but no trend observable. A comparison of our results to previous Fourier-transform infrared spectroscopy results [20] shows a good agreement of the transition frequencies for most transitions, given the limited resolution (75 MHz) and poorly defined pressures (0.5 to 4 mbar) of these measurements. The frequency difference between these results and ours is less than 3 MHz, except for one transition $((26,-7,2)\leftarrow(26,-8,2))$ with a deviation of 32.9 MHz. This is consistent with other works [10], showing similar differences to frequencies measured in [20].

　These results show that our method is able to characterize transitions with high precision and accuracy. The results include not only the rest frequency, but also the line strength, pressure broadening and pressure shift, which are currently missing in the JPL database. The setup that has been used in this work can further be improved to measure weaker transitions by increasing the length of the absorption cell or to perform Doppler-free spectroscopy, which would allow sub-Doppler resolution. A reduction of the leakage rate of the absorption cell would improve the precision of the rest frequencies as the uncertainties in pressure contribute the most to their uncertainties. Additionally, a reduction of measuring time by either a faster detector, ideally without the need for modulation, or a way to sweep the QCL frequency at a higher rate without losing the lock would further reduce these uncertainties.

**Table 1. Rest frequencies $f_{rest}$, quantum numbers, frequency differences to JPL $\Delta f$, frequency differences to [20] $\Delta f_M$, pressure shifts, transition strengths, and pressure broadening of the measured transitions between 3443.5 GHz and 3447.6 GHz. The uncertainties of $f_{rest}$ are given as the last two digits**

| Nr. | $f_{rest}$ (GHz) and transition quantum numbers (J,(±)K,(±)$\nu_t$) | $\Delta f$ (MHz) | $\Delta f_M$ (MHz) | Pressure shift (MHz/hPa) | Measured transition strength $\log_{10}(\text{nm}^2$ MHz) and acc. to [21] | Pressure broadening (MHz/hPa) |
|---|---|---|---|---|---|---|
| 1 | 3443.595183(22) (31,7,-1) ← (31,6,+1) | 0.693 | - | 0.7 ± 0 0.03 | -2.88 ± 0.01 -3.1521 | 15.7 ± 1.8 |
|  | 3443.595183(22) (31,7,+1) ← (31,6,-1) | -1.239 | - |  | -2.88 ± 0.01 -3.1521 |  |
| 2 | 3443.815112(50) (21,6,2) ← (20,7,1) | -5.688 | -1.583 | 1.5 ± 0.07 | -3.5 ± 0.2 -3.2455 | 20.9 ± 6.0 |
| 3 | 3444.061531(90) (29,-7,2) ← (29,-8,2) | 6.247 | - | - | -3.2 ± 0.3 -3.5215 | - |
| 4 | 3444.197570(29) (8,8,1) ← (9,9,0) | -0.232 | 1.038 | 0.09 ± 0.04 | -2.78 ± 0.08 -2.6525 | 16.7 ± 2.3 |
| 5 | 3444.404707(44) (3,1,+2) ← (4,0,+2) | 0.847 | 1.618 | 0.73 ± 0.07 | -2.9 ± 0.1 -2.9926 | 15.9 ± 2.1 |
| 6 | 3446.021342(24) (29,3,+1) ← (28,2,+1) | 0.796 | 2.071 | 0.89 ± 0.04 | -2.77 ± 0.09 -2.8571 | 15.2 ± 1.6 |
| 7 | 3446.346067(49) (27,-7,2) ← (27,-8,2) | 4.062 | -6.572 | 0.55 ± 0.06 | -3.4 ± 0.3 -3.3673 | 14.8 ± 4.9 |
| 8 | 3446.760926(09) (4,3,+2) ← (5,4,-1) | 0.564 | 2.667 | -0.31 ± 0.02 | -1.87 ± 0.02 -1.8806 | 16.8 ± 0.6 |
| 9 | 3447.379804(37) (21,8,1) ← (21,5,1) | 1.416 | - | -0.17 ± 0.05 | -2.92 ± 0.07 -3.1222 | 15.1 ± 1.5 |
|  | 3447.379804(37) (26,-7,2) ← (26,-8,2) | 0.612 | -32.902 |  | -2.92 ± 0.07 -3.2964 |  |
| 10 | 3447.438171(27) (19,10,+1) ← (18,9,+1) | 0.414 | 2.081 | 0.73 ± 0.04 | -2.34 ± 0.02 -2.2678 | 15.6 ± 1.3 |

## 4.   Summary

We performed precision spectroscopy with a phase-locked THz QCL to characterize several transition of methanol in the range of 3443.5 - 3447.6 GHz. We phase-locked the QCL to a reference signal based on a rubidium standard by downconverting the QCL emission using a harmonic Schottky diode mixer and an AMC. By changing the output frequency of the AMC we are able to sweep the QCL frequency as the IF stays fixed. This allows a frequency sweep over the total frequency range of the laser. The employed setup is compact and does not rely on liquid cryogens. We identified and quantified transition frequencies and broadening parameters of methanol in the range of 3443 to 3448 GHz. We found good agreement with current molecular database data for the stronger transitions, but substantial deviations for weaker transitions. Our findings might help to further improve current molecular models. Due to its compactness, similar setups might also be used in other laboratories for terahertz precision spectroscopy.

**Disclosures.** The authors declare no conflicts of interest.

**Data availability.** The data presented in this paper is available from the authors upon reasonable request.

**Supplemental document.** See Supplement 1 for supporting content.

## References

1. L. Consolino, F. Cappelli, M. S. de Cumis, *et al.*, "QCL-based frequency metrology from the mid-infrared to the THz range: a review," Nanophotonics **8**(2), 181–204 (2019).
2. H. Richter, C. Buchbender, R. Güsten, *et al.*, "Direct measurements of atomic oxygen in the mesosphere and lower thermosphere using terahertz heterodyne spectroscopy," Commun Earth Environ **2**(1), 19 (2021).
3. M. Wienold, A. D. Semenov, E. Dietz, *et al.*, "OSAS-B: A Balloon-Borne Terahertz Spectrometer for Atomic Oxygen in the Upper Atmosphere," IEEE Trans. Terahertz Sci. Technol. **14**(3), 327–335 (2024).
4. H.-W. Hübers, H. Richter, U. U. Graf, *et al.*, "Direct detection of atomic oxygen on the dayside and nightside of Venus," Nat. Commun. **14**(1), 6812 (2023).
5. H. V. L. Nguyen and I. Kleiner, "Understanding (coupled) large amplitude motions: the interplay of microwave spectroscopy, spectral modeling, and quantum chemistry," Physical Sciences Reviews **7**(6), 679–726 (2022).
6. F. Simon, C. Elmaleh, J. Decker, *et al.*, "Cavity assisted high-resolution THz spectrometer," Photonics and Nanostructures - Fundamentals and Applications **58**, 101227 (2024).
7. S. Bartalini, L. Consolino, P. Cancio, *et al.*, "Frequency-comb-assisted terahertz quantum cascade laser spectroscopy," Phys. Rev. X **4**(2), 021006 (2014).
8. L. Consolino, M. Nafa, M. de Regis, *et al.*, "Quantum cascade laser based hybrid dual comb spectrometer," Commun. Phys. **3**(1), 69 (2020).
9. L. Djevahirdjian, L. Lechevallier, M.-A. Martin-Drumel, *et al.*, "Frequency stable and low phase noise THz synthesis for precision spectroscopy," Nat. Commun. **14**(1), 7162 (2023).
10. M. De Regis, S. Bartalini, M. Ravaro, *et al.*, "Room-Temperature Continuous-Wave Frequency-Referenced Spectrometer up to 7.5 THz," Phys. Rev. Appl. **10**(6), 064041 (2018).
11. A. F. Krupnov, M. Tretyakov, S. P. Belov, *et al.*, "Accurate broadband rotational BWO-based spectroscopy," J. Mol. Spectrosc. **280**, 110–118 (2012).
12. L. Schrottke, M. Wienold, R. Sharma, *et al.*, "Quantum-cascade lasers as local oscillators for heterodyne spectrometers in the spectral range around 4.745 THz," Semicond. Sci. Technol. **28**(3), 035011 (2013).
13. H.-W. Hübers, H. Richter, and M. Wienold, "High-resolution terahertz spectroscopy with quantum-cascade lasers," J. Appl. Phys. **125**(15), 151401 (2019).
14. H. Richter, M. Wienold, L. Schrottke, *et al.*, "4.7-THz Local Oscillator for the GREAT Heterodyne Spectrometer on SOFIA," IEEE Trans. Terahertz Sci. Technol. **5**(4), 539–545 (2015).
15. S. A. Levshakov, M. G. Kozlov, and D. Reimers, "Methanol as a tracer of fundamental constants," The Astrophysical Journal **738**(1), 26 (2011).
16. X. Lü, B. Röben, V. Pistore, *et al.*, "Terahertz Quantum-Cascade Lasers: From Design to Applications," IEEE Trans. Terahertz Sci. Technol. **14**(5), 579–591 (2024).
17. D. Jayasankar, V. Drakinskiy, N. Rothbart, *et al.*, "A 3.5-THz, ×6-harmonic, single-ended Schottky diode mixer for frequency stabilization of quantum-cascade lasers," IEEE Trans. Terahertz Sci. Technol. **11**(6), 684–694 (2021).
18. H. Richter, N. Rothbart, M. Wienold, *et al.*, "Phase Locking of Quantum-Cascade Lasers Operating Around 3.5 and 4.7 THz With a Schottky-Diode Harmonic Mixer," IEEE Trans. Terahertz Sci. Technol. **14**(3), 346–353 (2024).
19. D. M. Slocum, L.-H. Xu, R. H. Giles, *et al.*, "Retrieval of methanol absorption parameters at terahertz frequencies using multispectral fitting," J. Mol. Spectrosc. **318**, 12–25 (2015).
20. G. Moruzzi, P. Riminucci, F. Strumia, *et al.*, "The spectrum of CH3OH between 100 and 200 cmi; Torsional and "forbidden" transitions," J. Mol. Spectrosc. **144**, 139–200 (1990).
21. H. M. Pickett, R. L. Poynter, E. A. Cohen, *et al.*, "Submillimeter, millimeter, and microwace spectral line catalog," J. Quant. Spectrosc. Radiat. Transfer **60**(5), 883–890 (1998).